Room temperature negative differential resistance characteristics of polar III-nitride resonant tunneling diodes

C. Bayram, Z. Vashaei, and M. Razeghi[a)]
Department of Electrical Engineering and Computer Science, Center for Quantum Devices, Northwestern University, Evanston, Illinois 60208, USA

(Received 19 July 2010; accepted 10 August 2010; published online 31 August 2010)

III-nitride resonant tunneling diodes (RTDs), consisting $Al_{0.2}Ga_{0.8}N/GaN$ double-barrier (DB) active layers, were grown on c-plane lateral epitaxial overgrowth (LEO) GaN/sapphire and c-plane freestanding (FS) GaN. RTDs on both templates, fabricated into mesa diameters ranging from 5 to 35 μm, showed negative differential resistance (NDR) at room temperature. NDR characteristics (voltage and current density at NDR onset and current-peak-to-valley ratio) were analyzed and reported as a function of device size and substrate choice. Our results show that LEO RTDs perform as well as FS ones and DB active layer design and quality have been the bottlenecks in III-nitride RTDs. © *2010 American Institute of Physics*. [doi:10.1063/1.3484280]

Negative differential resistance (NDR) is a quantum-physical phenomenon based on tunneling. NDR devices do not obey Ohm's Law which simply states current is proportional to the applied voltage. In NDR devices, under a specific operation range, current through the device decreases with increase in voltage. This creates an effective negative resistance over the specific operation range that is benefited in many circuit elements (such as oscillators, amplifiers, and frequency converters) and employed in many electronic devices (such as radios).

Resonant tunneling diodes (RTDs), compared to other NDR devices such as (Esaki) tunnel and transferred-electron devices (i.e., Gunn diode, thyristor, and impact ionization avalanche transit-time diode), possess lower junction capacitance (due to relatively lower doping levels) enabling them generate and detect terahertz (THz) waves.[1] The current bottlenecks of conventional (CONV.) (such as GaAs-based) RTDs are the upper frequency limit, output power/detection sensitivity and operating temperature.[1]

Recently, III-nitrides have gained interest for RTDs. Wide band gap, large conduction band discontinuity [~2.1 eV in AlN/GaN (Ref. 2)], high carrier mobility and thermal stability promise high power high frequency room temperature (RT) operation. Various groups have studied $Al_XGa_{(1-X)}N/GaN$ ($X \geq 0.70$) double-barrier (DB) resonant tunneling structures.[3–10] However, in these studies, after the initial I-V measurements, the NDR degraded leaving dominant exponential I-V behavior in the consequent ones. Recently, we have shown reliable and reproducible NDR in GaN RTDs employing low aluminum content active layer design.[11] Our demonstration motivates further research into RTDs employing low aluminum content active layers for improved reliability and reproducibility. Demonstrating NDR and understanding transport in III-nitride RTDs will enable RT THz oscillators and pave the way toward RT THz quantum cascade lasers.[12]

The main purpose of this work is to study the NDR characteristics (voltage and current density at NDR onset and current-peak-to-valley ratio) in RTDs grown on lateral epitaxial overgrowth (LEO) GaN/sapphire [dislocation density (DD) $< 5 \times 10^7$ cm^{-2}][8] and freestanding (FS) GaN (DD $< 1 \times 10^6$ cm^{-2}). Low aluminum content (20%) AlGaN barrier was employed to form DB active layer to minimize active layer-related dislocations and polarization fields. Area-dependency of NDR characteristics were realized by fabricating RTDs with various mesa diameters (from 5 to 35 μm). By correlating substrate choice and mesa-size-dependency with NDR characteristics, the bottlenecks in achieving reliable polar III-nitride RTDs were investigated.

The RTDs were grown in an AIXTRON 200/4-HT horizontal flow low-pressure metal organic chemical vapor deposition reactor. Trimethlyaluminum and trimethylgallium were used as the metal organic precursors for Al and Ga, respectively. Silane was used as the *n*-type dopant source. Ammonia and hydrogen/nitrogen mixture[9] were used as the anion source and carrier gas, respectively. Independent growths and Hall-effect measurements determined *i*-and *n*-GaN carrier concentrations as 6×10^{16} cm^{-3} and 3×10^{19} cm^{-3}, respectively.[9]

The growth of the FS RTDs started with conditioning of c-GaN substrate followed by 3 μm *i*-GaN. Along with FS GaN template, we loaded our high quality LEO GaN (Ref. 13) templates for device regrowth. First, 750 nm thick *n*-GaN was grown to act as bottom contact. The active layer of a DB RTD is composed of a narrower band gap material sandwiched between wider band gap materials; thus, an inherit lattice mismatch between materials is inevitable. The critical thickness (above which dislocations are generated) is inversely proportional to aluminum content for GaN homoepitaxial growth.[14] Thus, our RTD active layer employs low aluminum content (20%) in the barrier to prevent the lattice relaxation via dislocation formation as the barrier is grown thinner (1.5 nm) than the critical thickness (~1.8 nm).[14] The RTD active layer, composed of 2.0 nm *i*-GaN, 1.5 nm *i*-$Al_{0.20}Ga_{0.80}N$, 1.25 nm *i*-GaN, 1.5 nm *i*-$Al_{0.20}Ga_{0.80}N$, and 2.0 nm *i*-GaN, was employed. This arrangement enables a conduction band offset of 0.42 eV in AlGaN barrier, giving a single and discreet electronic level (E) of 0.32 eV in the GaN well. The device was finalized via top contact layer of 450 nm thick *n*-GaN.

Fabrication of RTDs was realized via CONV. semiconductor methods and tools.[8,11] First, top mesas were formed

[a)]Electronic mail: razeghi@eecs.northwestern.edu.

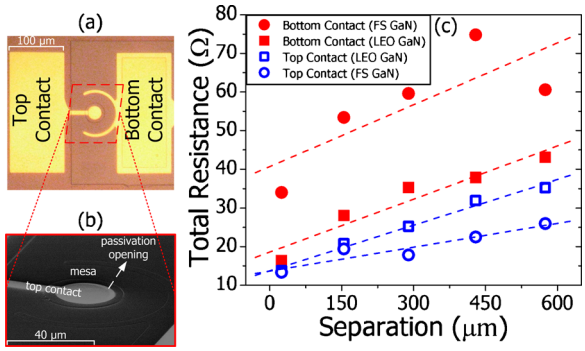

FIG. 1. (Color online) (a) Top-view optical micrograph of a fabricated RTD device, (b) SEM bird's eye view of a fabricated RTD mesa (zoomed-in), and (c) TLM measurements of top and bottom contacts of RTDs grown on LEO and FS GaN (each dashed line is the linear fitting to the respective TLM measurement).

by dry etching. Then, the bottom contact metal of 400 Å Ti/1500 Å Au was deposited. This was followed by deposition of 300 nm thick silicon dioxide as passivation. This passivation layer was removed from the top contact region of device mesa and bottom contact pads via wet-etching to form passivation opening. The RTD was completed by 400 Å Ti/1500 Å Au top contact metal deposition that formed the top contact bridge to the device mesa and top contact pads. Figure 1(a) shows the top optical microscope view of fabricated RTD device. The mesa is connected to the top contact pads via bridge structure. Bottom contact is surrounding the mesa partly to enable efficient carrier injection [Figs. 1(a) and 1(b)]. Figure 1(b) shows the bird's eye view of the mesa region under scanning electron microscope (SEM).

Figure 1(c) shows the transmission line model (TLM) measurements of top and bottom contacts of RTDs grown on LEO and FS GaN. Each dashed line [in Fig. 1(c)] is the linear fitting to the respective TLM measurement set. The linear behavior of total resistance as a function of TLM contact separation proves that top and bottom contacts of RTDs are Ohmic for both (LEO and FS GaN) templates. From the linear fittings [Fig. 1(c)], the top (ρ_C^{TOP}) and bottom specific contact resistances (ρ_C^{BOTTOM}) are determined as 2.76×10^{-3} (5.22×10^{-3}) $\Omega\,cm^2$, and 4.36×10^{-3} (17.81×10^{-3}) $\Omega\,cm^2$ leading to a total resistance R_T^{LEO} (R_T^{FS}) of 33.4(104.7) Ω for LEO (FS) GaN RTDs. The effects of differences in R_T on NDR behavior will be addressed in the electrical measurements.

RTD electrical measurements were realized under continuous wave at RT. The voltage polarity refers to that applied to the top contact. All I-V curves were measured using an HP4155A semiconductor parameter analyzer configured to input a voltage sweep while measuring current.

Figures 2(a)–2(c) plots I-V characteristic of the RTDs with mesa diameters of (a) 7, (b) 9, and (c) 35 μm grown on LEO and FS GaN. For comparison with RTDs on CONV. GaN/sapphire (i.e., 2 μm thick-GaN on c-sapphire; DD $\approx5\times10^8$ cm^{-2}), Fig. 2(c) includes I-V curve of an RTD on CONV. GaN. The onset voltage of NDR (V_{NDR}), was observed to be independent of mesa size, and is ~1.19 (±0.11) V and 1.49 (±0.18) V for LEO and FS RTDs, respectively. The slight difference between V_{NDR}^{LEO} and V_{NDR}^{FS} is due to the difference in device resistances [33.4 Ω (LEO RTDs) versus 104.7 Ω (FS RTDs)]. For the experimented $Al_{0.2}Ga_{0.8}N$ (1.5 nm)/GaN (1.2 nm)/$Al_{0.2}Ga_{0.8}N$ (1.5 nm) active layer, the electronic energy level (E) and Fermi energy level (E_F) (reference to conduction band) are calculated as 0.32 eV and 67 meV leading to NDR voltage of ~0.51 V ($V_{NDR}\cong2\times(E-E_F)/e$) under ideal conditions. The difference between the observed and ideal V_{NDR} is attributed to voltage drop due to the series resistance and polarization charges at the $Al_{0.2}Ga_{0.8}N/GaN$ interfaces.[15] For all mesa sizes [Figs. 2(a)–2(c)], current-peak-to-valley-ratios (CPVR) of LEO RTDs were comparable to those of FS GaN showing the promise of LEO GaN template for RTD studies. The CONV. RTDs also showed similar characteristics to LEO RTDs; however, after the initial I-V curve, their CPVR decreased significantly and (after third scan) eventually disappeared. For LEO and FS RTDs, NDR characteristics were stable for around 20 scans with no significant degradation. The significant reliability difference between CONV. RTDs and LEO/FS RTDs is attributed to high density of threading dislocations leading to trapping and scattering in the former case.

Thanks to the reproducibility of NDR behavior in LEO RTDs, effects of I-V curve measurement conditions [voltage sweep steps of 5 and 20 mV, and integration times of 640 μs (short), 16.7 ms (medium), and 266 ms (long)] were studied. Figure 3 plots the I-V curves of an RTD under various measurement conditions. No significant variance was observed in V_{NDR} and CPVR between voltage sweep steps of 5 and 20 mV and speeds of short and medium. However, for the long integration time, V_{NDR} and CPVR decreased that is attributed to too much averaging of current. Figure 3 inset shows (under optimized measurement conditions) the I-V curve of an RTD demonstrating NDR under both reverse and forward biases. Due to the (asymmetrical) polarization charges at the AlGaN/GaN interface,[15] the V_{NDR} under reverse bias is smaller than that under forward bias in harmony with the

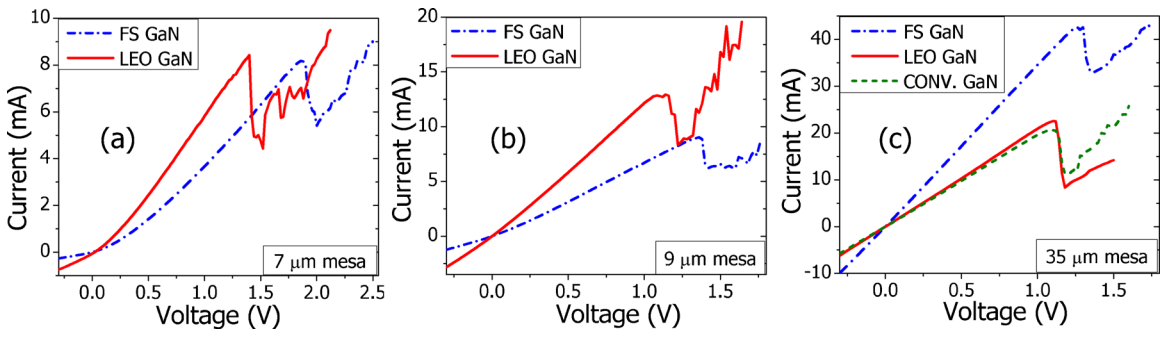

FIG. 2. (Color online) Electrical (I-V curve) measurements of RTDs grown on LEO GaN and FS GaN for various mesa diameters: (a) 7 μm, (b) 9 μm, and (c) 35 μm. For comparison, I-V curve of (35 μm in. diameter) RTD grown on CONV. GaN/sapphire is appended to Fig. 2(c).

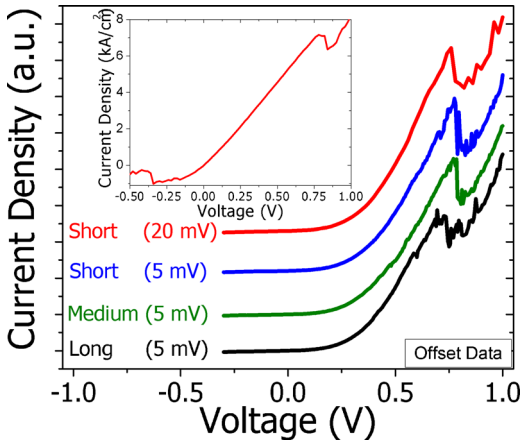

FIG. 3. (Color online) Electrical measurements (I-V curves) of RTDs under various measurement conditions [integration times of 640 μs (short), 16.7 ms (medium), and 266 ms (long), and voltage sweep widths of 5 and 20 mV]. Inset shows the I-V curve of an RTD demonstrating NDR under both reverse and forward biases.

theory[16] and experimental low temperature (at ~4 K) demonstrations.[4] Demonstration of NDR under both biases and at RT shows the overall quality of the LEO RTDs.

Figure 4 shows current density at the onset of NDR as a function of mesa diameter for LEO and FS RTDs. Ten devices per diameter per template were averaged, and average current density value (J_{NDR}) along with the standard error were plotted. With increasing mesa diameter, the J_{NDR} decreased for both substrates. The high J_{NDR} for smaller devices could be explained by a reduced effective area contributing to the resonant tunneling current, due to material inhomogeneities. These inhomogeneities could arise from dislocations,[8] aluminum interdiffusion[9] and interface roughness between AlGaN barrier and GaN well and polarization charges[15] at the active layer interfaces. This also explains why LEO RTDs possessed a higher J_{NDR} than FS GaN as FS GaN (Ref. 11) has lower dislocation density and is more uniform than LEO GaN (Refs. 8 and 9) leading to a lower J_{NDR} in FS RTDs. With increasing mesa diameter, the effective area contributing to the resonant tunneling current increases that decreases J_{NDR}. For larger diameters, J_{NDR} is less

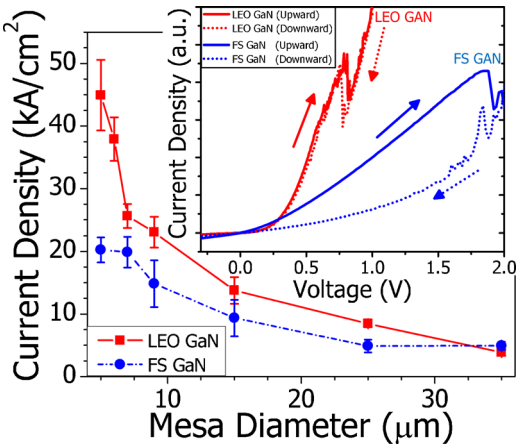

FIG. 4. (Color online) Dependence of J_{NDR} on the RTD mesa diameter. Inset shows the electrical hysteresis measurements of LEO and FS RTDs. The hysteresis curves are realized via measuring the device I-V from negative to positive voltage followed by positive to negative voltage–a loop of electrical I-V measurements.

sensitive to area and substrate choice, and on the order of ~4.34 kA/cm^2–comparable to earlier works.[10,11]

For hysteresis measurements (i.e., difference in I-V behavior between upward and downward scan, seen in Fig. 4 inset), the voltage sweep was adjusted for a loop. The hysteresis in V_{NDR} and J_{NDR} identified in the I-V curve (Fig. 4 inset) is attributed to charge trapping associated with defects. Charge trapping during the upward scan broadens the discrete electronic state in the well decreasing the V_{NDR} in the downward scan. Observations of NDR under both upward and downward scans [as opposed to earlier works[3–10] employing high aluminum content active layers ($X \geq 0.70$)] suggest LEO and FS RTDs are high quality[1] and that the low aluminum content active layer is crucial in the stability of NDR behavior.[11]

In conclusion, the stability of NDR in III-nitride RTDs can be increased by minimizing the template dislocation density and lowering aluminum content in the active layer. Under optimized measurement conditions, V_{NDR} was shown to be lower under reverse bias and downward scan than under forward bias and upward scan; attributed to polarization charges and defect charging, respectively. High quality LEO GaN was shown to be a good alternative to FS GaN in RTD studies. Our results motivates for further research toward low aluminum content tunneling structures that can be employed in THz optoelectronic devices.

The authors acknowledge Dr. J. Zavada of ARO, Dr. J. Mangano and Dr. Scott Rodgers of DARPA, and Mr. Jerry Speer of U.S. Army RDECOM for their interest and encouragement.

[1]M. Asada, S. Suzuki, and N. Kishimoto, Jpn. J. Appl. Phys. **47**, 4375 (2008).
[2]G. Martin, S. Strite, A. Botchkarev, A. Agarwal, A. Rockett, H. Morkoc, W. R. L. Lambrecht, and B. Segall, Appl. Phys. Lett. **65**, 610 (1994).
[3]A. Kikuchi, R. Bannai, K. Kishino, C. M. Lee, and J. I. Chyi, Appl. Phys. Lett. **81**, 1729 (2002).
[4]C. T. Foxon, S. V. Novikov, A. E. Belyaev, L. X. Zhao, O. Makarovsky, D. J. Walker, L. Eaves, R. I. Dykeman, S. V. Danylyuk, S. A. Vitusevich, M. J. Kappers, J. S. Barnard, and C. J. Humphreys, Phys. Status Solidi C **0**, 2389 (2003).
[5]M. Hermann, E. Monroy, A. Helman, B. Baur, M. Albrecht, B. Daudin, O. Ambacher, M. Stutzmann, and M. Eickhoff, Phys. Status Solidi C **1**, 2210 (2004).
[6]M. V. Petrychuk, A. E. Belyaev, A. M. Kurakin, S. V. Danylyuk, N. Klein, and S. A. Vitusevich, Appl. Phys. Lett. **91**, 222112 (2007).
[7]S. Leconte, S. Golka, G. Pozzovivo, G. Strasser, T. Remmele, M. Albrecht, and E. Monroy, Phys. Status Solidi C **5**, 431 (2008).
[8]C. Bayram, Z. Vashaei, and M. Razeghi, Appl. Phys. Lett. **96**, 042103 (2010).
[9]Z. Vashaei, C. Bayram, and M. Razeghi, J. Appl. Phys. **107**, 083505 (2010).
[10]S. Golka, C. Pflugl, W. Schrenk, G. Strasser, C. Skierbiszewski, M. Siekacz, I. Grzegory, and S. Porowski, Appl. Phys. Lett. **88**, 172106 (2006).
[11]C. Bayram, Z. Vashaei, and M. Razeghi, Appl. Phys. Lett. (unpublished).
[12]V. D. Jovanović, D. Indjin, Z. Ikonic, and P. Harrison, Appl. Phys. Lett. **84**, 2995 (2004).
[13]C. Bayram, J. L. Pau, R. McClintock, and M. Razeghi, Appl. Phys. B: Lasers Opt. **95**, 307 (2009).
[14]A. D. Bykhovski, B. L. Gelmont, and M. S. Shur, J. Appl. Phys. **81**, 6332 (1997).
[15]F. Sacconi, A. D. I. Carlo, and P. Lugli, Phys. Status Solidi A **190**, 295 (2002).
[16]S. N. Grinyaev and A. N. Razzhuvalov, Semiconductors **37**, 433 (2003).